

<https://doi.org/10.1038/s44385-025-00009-x>

Stick-and-play bioadhesive hairlike electrodes for chronic EEG recording on human



Salahuddin Ahmed^{1,9}, Marzia Momin^{1,9}, Jiashu Ren¹, Hyunjin Lee², Basma AlMahmood³, Li-Pang Huang⁴, Archana Pandiyan⁵, Loganathan Veeramuthu⁵, Chi-Ching Kuo⁵✉ & Tao Zhou^{1,2,6,7,8}✉

Chronic high-fidelity electroencephalogram (EEG) recording faces challenges due to weak EEG signals and presence of hair, which create interfacial gaps and motion artifacts. To ensure reliable EEG recording, stable connection between electrodes and the scalp is essential. Metallic electrodes with electrolyte gel are commonly used, but their stability is often affected by gel drying and inconsistent electrode positioning across sessions. Here, we report stick-and-play hairlike device that can attach to the human scalp without the need for skin preparation, using a highly flexible and stretchable electrode material and robust bioadhesive material. The hairlike device can be worn for long term without being noticeable, maintaining a stable skin adhesion and interface impedance across different recording sessions and hundred cycles of cyclic loading. The design, which mimics human hair, makes it indistinguishable from a natural look. Additionally, the hairlike device has been demonstrated as an efficient medium for long-term, high-quality EEG recordings.

Electroencephalography (EEG), a non-invasive approach for brain activity monitoring, enables the rapid investigation of physiological conditions and dysfunctions of the human brain with high temporal resolution, which is essential for clinical diagnostics, therapeutics, and neuroscience research^{1–3}. In addition, chronic reliable EEG recording is of great importance for clinical applications such as seizure monitoring, the evaluation of sleep disorders, cerebrovascular disease, psychiatric conditions, and movement disorders⁴. However, reliable EEG recording is challenging due to the weak nature of EEG signal⁵ and the presence of thick hair on the scalp which induces interfacial gaps between the scalp and recording electrodes^{6,7}. This leads to fluctuations in interfacial impedance between the electrode and the skin⁸. For high-quality EEG recording, good conformality and favorable mechanical interaction with human skin tissue on the scalp are very important^{2,9}.

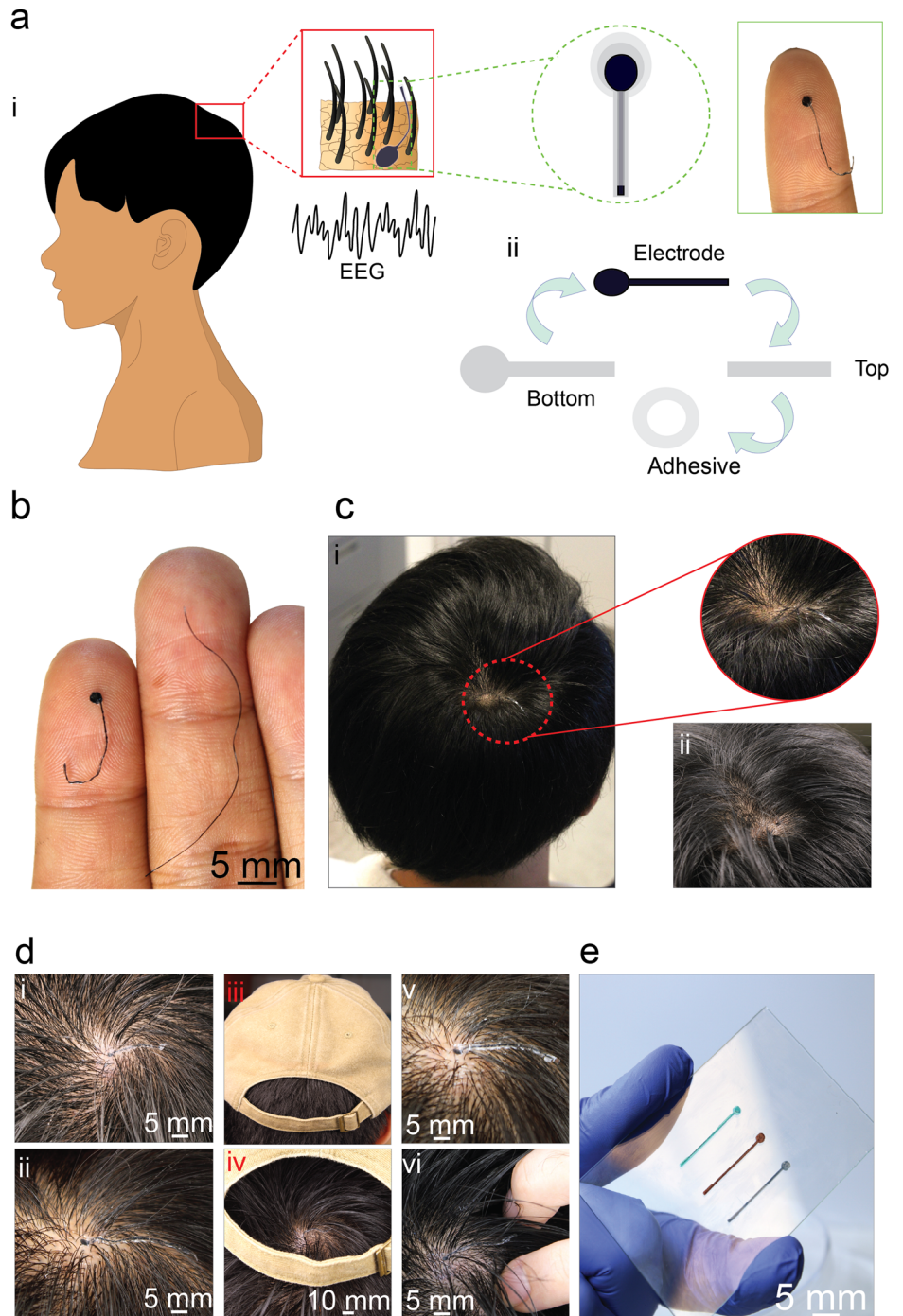
Traditional EEG systems typically employ gold cup electrodes or Ag/AgCl wet electrodes, which require the application of conductive gels to maintain proper contact with the scalp. These systems have been widely used in clinical and research settings due to their ability to capture EEG signals from the brain¹⁰. Although wet electrodes are often regarded as the

benchmark for EEG monitoring, they encounter certain obstacles that restrict their practicality and user comfort. An important concern is the discomfort¹¹ caused by the electrodes, especially when they must be worn for long durations. The application of conductive gels can be messy and time-consuming, and the gels tend to dry out over time, necessitating frequent reapplication to maintain signal quality^{12,13}. This reapplication process can be inconvenient and intrusive, particularly in long-term monitoring scenarios. Moreover, the rigid nature of these electrodes can cause signal instability due to movement. Any slight displacement or movement of the electrodes can lead to significant artifacts and noise in the recorded signals, compromising the accuracy and reliability of the data. This instability is particularly problematic in studies where subjects are required to perform physical activities. Furthermore, their chronic reliability and stability is compromised by the drying of the conductive gels and inconsistency in electrode positions across different recording sessions. Additionally, the potential for skin irritation from the application of gels further reduces the feasibility of traditional EEG systems for continuous, long-term use.

Leveraging the highly flexible and stretchable nature, along with the low mechanical modulus of our electrode material, combined with the

¹Department of Engineering Science and Mechanics, The Pennsylvania State University, Pennsylvania, USA. ²Department of Biomedical Engineering, The Pennsylvania State University, Pennsylvania, USA. ³Department of Physics, The Pennsylvania State University, Pennsylvania, USA. ⁴Department of Biology, The Pennsylvania State University, Pennsylvania, USA. ⁵Department of Molecular Science and Engineering, National Taipei University of Technology, Taipei, Taiwan. ⁶Center for Neural Engineering, The Pennsylvania State University, Pennsylvania, USA. ⁷Huck Institutes of the Life Sciences, The Pennsylvania State University, Pennsylvania, USA. ⁸Materials Research Institute, The Pennsylvania State University, Pennsylvania, USA. ⁹These authors contributed equally: Salahuddin Ahmed, Marzia Momin. ✉e-mail: kuocc@mail.ntut.edu.tw; tzz5199@psu.edu

Fig. 1 | Bioadhesive hairlike electronics for stable chronic EEG monitoring. **a** (i) Schematic illustration of bioadhesive hairlike electrodes for stable chronic EEG recording from a hairy scalp. (ii) Different components of hairlike electrodes: PDMS bottom and top layer, conductive polymer-based electrode, and bioadhesive layer. **b** Photograph of a hairlike electrode (left) and a human hair (right) (scale bar-5 mm). **c** (i) Photograph of a hairlike electrode placed on the scalp. (ii) The device remains invisible on the scalp, owing to its biomimetic natural appearance. **d** Stable adhesion of hairlike electrodes under various conditions: Hairlike electrode before (i) and after (ii) workout, illustrating the device's stability in the presence of scalp sweat (scale bar-5 mm). (iii) The ability to withstand complications of wearing a cap. (iv) Stably stay on the scalp during cap removal (scale bar-10 mm). (v and vi) Device enduring the force exerted during hair combing with hands (scale bar-5 mm). **e** Hairlike devices available in different hair colors, allowing for seamless integration with various hair types without cosmetic differences (scale bar-5 mm).



robust adhesion properties of a bioadhesive component, we have developed a stick-and-play hairlike device for stable chronic EEG monitoring. This device can be attached to the human scalp without the need for conductive electrolyte gel application. The device is designed to be exceptionally thin, lightweight, and highly conformable to the scalp, offering a more comfortable and stable interface for EEG recordings. The bioadhesive material's exceptional adhesion properties contribute to the formation of a robust interface between the recording electrodes and the scalp. This ensured a stable positioning of the electrodes, allowing for continuous and comfortable wearing of the hairlike device without the risk of peeling off or skin irritation. We designed the hairlike device to mimic human hair, enabling wearers to use it inconspicuously without social stigma or feelings of alienation. This discreet integration into daily life is particularly beneficial for

individuals who require continuous EEG monitoring, such as those with epilepsy or other neurological conditions. Owing to strong adhesion, the hairlike device achieves conformal contact with the skin on hairy scalp which contributes to the long-term high-fidelity EEG recording over continuous wearing of the device without the need for additional steps to secure the device continuously.

Results

3D printed hairlike device

To fabricate the hairlike EEG recording device, we utilized direct ink writing (DIW) 3D printing¹⁴, a versatile technique that allows precise patterning of various inks through controlled nozzle movement in three-dimensional, building the device layer by layer¹⁵. This method offers high spatial

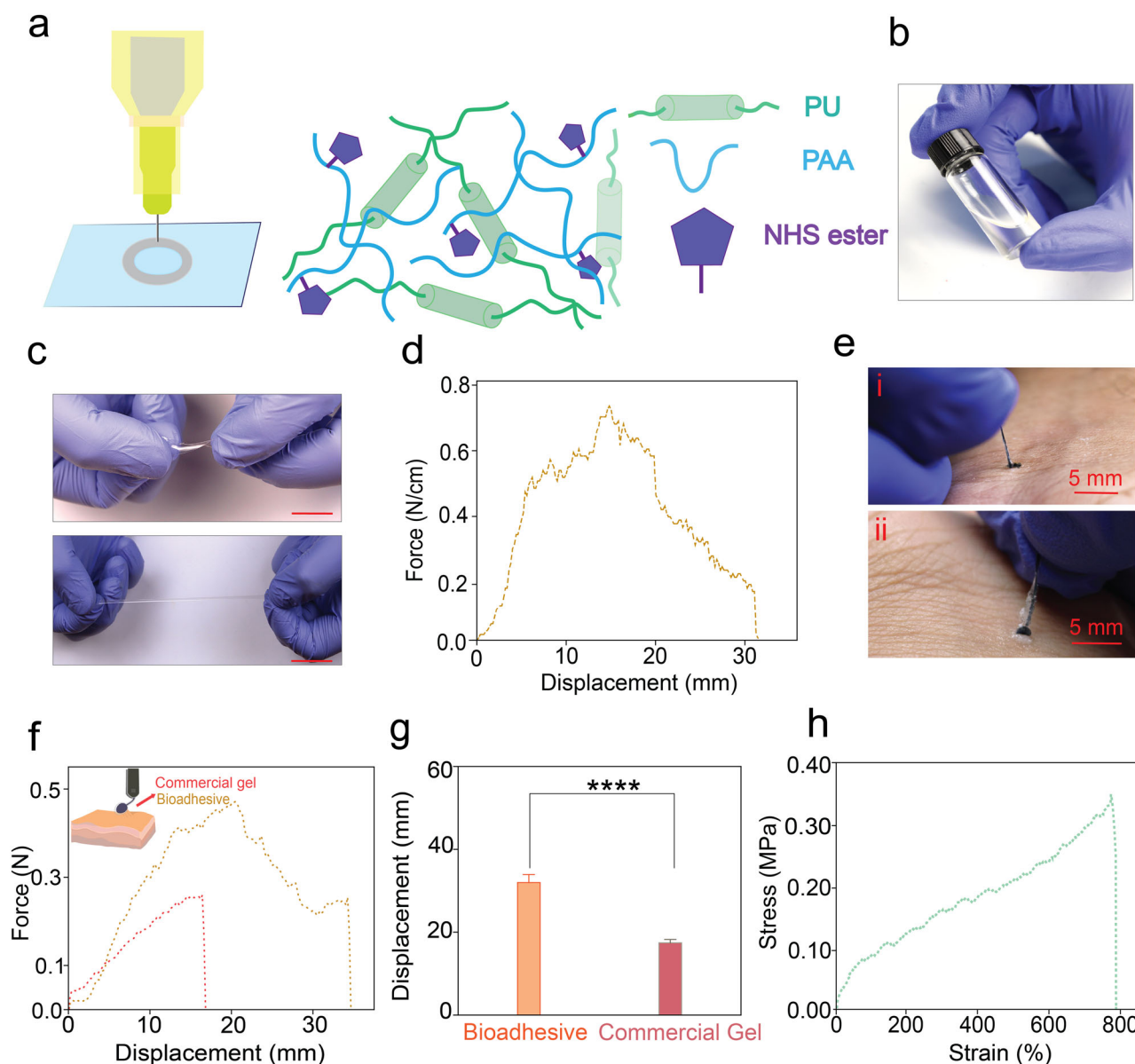


Fig. 2 | Bioadhesive materials for hairlike electrodes. **a** Schematic illustration of bioadhesive material and its 3D printing. **b** Photograph of bioadhesive ink for 3D printing. **c** Photographs of printed bioadhesive in twisted (top) and stretched (bottom) form. (Scale bar- 4 cm) **d** Interfacial adhesion force of the bioadhesive on skin. **e** Photographs highlighting comparison of the adhesion of device on skin using the developed bioadhesive material (i) and commercial EEG gel (ii). **f** Adhesion force

of hairlike device with bioadhesive and commercial EEG gel. **g** Plot for the comparison of adhesion force of hairlike device with bioadhesive and commercial EEG gel ($n = 4$). Statistical significance and P values are determined by two-sided unpaired t-test; **** $P < 0.0001$. Errors bars indicate standard deviation. **h** Experimental stress strain curve of 3D printed dog-bone shaped specimen of bioadhesive material.

resolution, reduced time in device fabrication, and excellent reproducibility, making it an ideal methodology for constructing intricate, multi-layered structures with the precision required for our application. We employed conducting polymer hydrogel material for the electrode layer which consists of poly(3,4-ethylenedioxythiophene): polystyrene sulfonate (PEDOT: PSS) and hydrophilic polyurethane (PU). This hydrogel material exhibits high electrical conductivity ($>11 \text{ Scm}^{-1}$)¹⁶ and high stretchability ($\sim 400\%$)¹⁶ ensuring optimal properties for our designed hairlike devices. Structurally, the hairlike device is composed of four layers (Fig 1a (ii)): the central conducting polymer hydrogel electrode layer is sandwiched between two PDMS encapsulation layers. The electrode layer has 3 components: The interface, the interconnect and the output unit. At the interface site, a single PDMS layer is used to expose the electrode, allowing it to directly acquire signals from the scalp. Additionally, an adhesive layer is printed around the

electrode layer on top of the bottom PDMS layer to secure the device in place.

We designed the hairlike device with the intention that it can be worn continuously over extended periods, allowing subjects to maintain their daily routines without experiencing any interference or noticeable cosmetic differences. The interface part of the hairlike device that adheres to the scalp is circular with a diameter of 1.5 mm, optimizing contact with the skin with minimal intrusiveness. The interconnect part of the device is designed to be 300 μm in width, providing a thin, hairlike structure that seamlessly integrates with the natural hair (Fig. 1b). This slender design minimizes any aesthetic impact and ensures the device's lightweight and flexible nature, enhancing user comfort. Upon placement, the device meshes naturally with the hair, becoming virtually invisible and preserving the

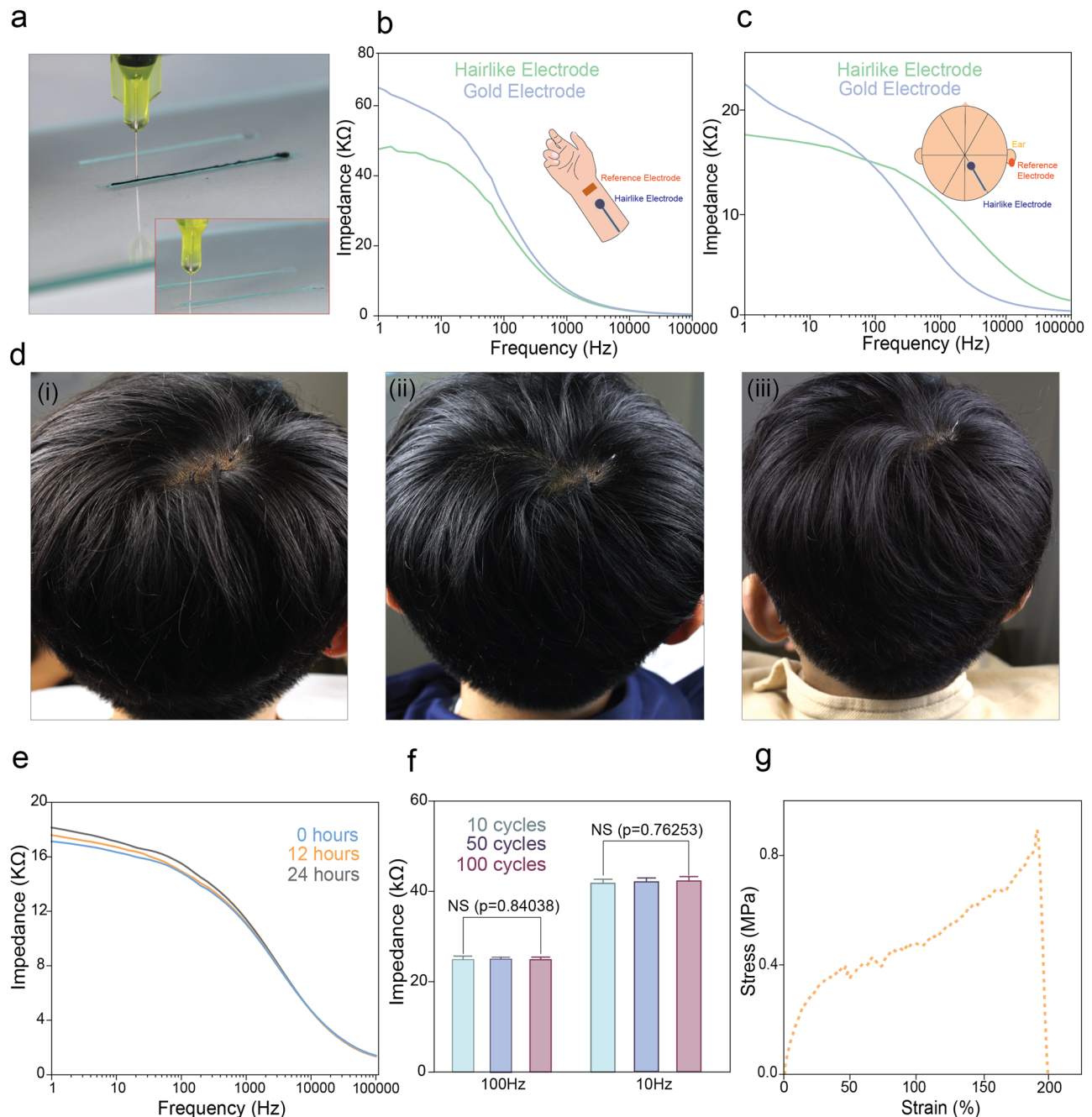


Fig. 3 | Printing of hairlike electrodes and characterization of their stability, electrical and mechanical properties. **a** Photographs of layer-by-layer printing process of hairlike electrodes with 100 μm nozzle using DIW-based multi-material 3D printing. **b** Impedance spectra of electrode-skin interface of hairlike electrodes and commercial gold electrodes on wrist. **c** Impedance spectra of electrode-skin interface of hairlike electrodes and commercial gold electrodes on hairy scalp. **d** Long-term stability assessment of the hairlike electrodes on a hairy scalp with

continuous wearing. Images depict the electrode on the scalp at 0 hours (i), 12 hours (ii), and 24 hours (iii), illustrating its durability over time. **e** Impedance spectra of the electrode-skin interface for the hairlike device at different time intervals: initially, after 12 hours, and after 24 hours of continuous wear on hairy scalp. **f** Plots for electrode skin impedance at 10 Hz and 100 Hz after different tensile cycles of hairlike electrodes. ($n = 4$) Error bars indicate standard deviation. **g** Engineering stress vs engineering strain curve for a hairlike electrode.

user's natural appearance (Fig. 1c). This design aspect is essential for user acceptance, as it allows the device to be worn discreetly in various social and professional settings without attracting notice. In addition to cosmetic advantages, the hairlike design ensures that the device does not interfere with daily activities. Its strong adhesion and flexibility allow it to remain robustly in place during movement, exercise, and routine hair grooming (Fig. 1d). To cater for subjects with different hair colors, we also designed the hairlike device for various hair colors (Fig. 1e) by adopting biocompatible dyes in the printing material (see Methods for detailed procedure).

3D printable adhesive ink

The bioadhesive was synthesized using a UV-assisted polymerization method (see Methods for detailed procedure). A solution containing PU, ethanol, deionized water, acrylic acid, α -ketoglutaric acid, and benzophenone was exposed to UV light. In this process, α -ketoglutaric acid initiated the polymerization of acrylic acid, while benzophenone generated radical sites in the PU, facilitating the covalent bonding of poly(acrylic acid) (PAA). The resultant PAA-integrated PU was then purified through dialysis in ethanol and water sequentially to remove any unreacted reagents, followed by thoroughly drying. To convert the synthesized PAA-integrated PU into a

printable ink, we dissolve it in an aqueous ethanol solution. N-(3-dimethylaminopropyl)—N-ethylcarbodiimide hydrochloride (EDC) and N-ethyl-N'-(, N-hydroxysuccinimide) (NHS) were introduced in the solution to introduce NHS ester functional groups on the PAA chains (Supplementary Fig. 1). The introduction of NHS esters significantly enhances the adhesive properties of the polymer by increasing its reactivity with amine groups present in proteins and other biomolecules. This increased reactivity facilitates the formation of strong and durable covalent bonds^{17,18}, making the adhesive highly effective for biological applications. The covalent bonding ensures robust attachment of hairlike device to the skin. Prior to 3D printing the solution was blended with PU to finely adjust its viscosity to enable high-resolution 3D printing¹⁹.

The rheological properties of the as developed bioadhesive exhibits a shear thinning behavior (Supplementary Fig. 2), which is characteristic of non-Newtonian fluids. For direct-ink-write (DIW) printing, the ink must flow smoothly through the nozzle under pressure and exhibit rapid recovery to its original shape post-extrusion. The rapidly reduced viscosity at higher shear rate enables the ink to flow easily through the fine nozzle under pressure, minimizing the risk of nozzle clogging and enabling a continuous, uninterrupted flow. High viscosity at low shear rate makes the material resistant to spreading upon printing, allowing precise printing of the adhesive layer of hairlike device.

To measure the adhesion performance of the bioadhesive to the skin surface, we measured the interfacial adhesive force between the bioadhesive and skin. The bioadhesive showed favorable adhesion to the skin surface with an average adhesion force of 0.7 N/cm (Fig. 2d). Owing to a high density of charged carboxylic acid groups, PAA chains can quickly consolidate with tissue surfaces to form intermolecular hydrogen bonds. Reactive NHS ester groups further enhance tissue adhesion by interacting with primary amines on tissue surfaces to form covalent amide bonds¹⁷. Hydrophilic PAA chains enhance rapid interfacial water absorption¹⁸, allowing the bioadhesive to maintain strong adhesion to the skin even during exposure to water, such as during showers, or when sweat forms on the scalp during exercise. We also evaluated the adhesion performance of the hairlike device using bioadhesive in comparison to a commercial adhesive EEG paste (Fig. 2e). The hairlike device with the bioadhesive demonstrated significantly stronger and more durable adhesion to the skin surface compared to the commercial adhesive EEG paste (Fig. 2 f-g). The bioadhesive showed adhesion performance which is almost double the strength of commercial EEG gel ($n = 4$) (Fig. 2g). The bioadhesive exhibited mechanical robustness with high flexibility and stretchability, allowing for seamless integration with nonplanar skin surfaces. The bioadhesive can be stretched about eight times of its original length with a Young's modulus of 42 kPa (Fig. 2h), which is comparable to that of the native tissue of muscle and skin²⁰. The low modulus of the bioadhesive ensures conformal contact with the curved surface of the skin, enhancing comfort. Additionally, it can be removed without causing any damage to the skin. The AFM image (Supplementary Fig. 3) of the bioadhesive post-attachment to human skin reveals a smooth surface with no residue left on the bioadhesive after removal.

Electrical and mechanical performance of hairlike device

An intimate interface between the electrode of the hairlike device and the skin is necessary for electrical communication. Leveraging the highly robust nature of the bioadhesive, we were able to establish a stable interface between the electrode and the skin. To evaluate their interface, we conducted electrochemical impedance spectroscopy (EIS) characterization of the hairlike device to study the interfacial impedances of the device electrode and skin on both the wrist and the scalp. For comparative analysis, we also measured the skin impedance using a gold electrode with commercial EEG paste. The bioadhesive's robust adhesion and the hydrogel electrode's flexibility facilitated conformal contact with the skin tissue. Consequently, the hairlike device demonstrated a lower electrode-skin electrical impedance compared to the commercial gold electrode. Specifically, the hairlike device exhibited skin impedances of 26.02 k Ω at 100 Hz and 43.89 k Ω at 10 Hz on the wrist

(Fig. 3b). On the scalp, the hairlike device showed impedances of 14.83 k Ω at 100 Hz and 16.72 k Ω at 10 Hz (Fig. 3c). The hairlike electrode also showed a high charge storage capacity (Supplementary Fig. 4).

To ensure the hairlike device is unobtrusive and does not interfere with daily activities, we tested its long-term adhesion and electrical performance. The device was placed on the scalp of a subject who then proceeded with their normal daily activities. We tested the placement and the adhesion performance of the device, which remained securely attached to the scalp for 24 hours (Fig. 3d). We also performed electrochemical impedance spectroscopy (EIS) characterization to determine interfacial impedances of the device electrode and skin on the scalp after 12 and 24 hours of continuous wear. The results showed that the impedance remained stable with no noticeable increase after 12 and 24 hours (Fig. 3e and Supplementary Fig. 5). These findings underscore the hairlike device's potential for long-term high-fidelity electrophysiological recordings, as evidenced by its lower impedance values and stable skin-electrode interface.

Before 3D printing, we have tested rheological behavior of all the components of hairlike electrode. Rheology characterizations (Supplementary Fig. 6) reveal that both the PDMS ink and the PEDOT:PSS electrode ink demonstrate shear-thinning behavior, where viscosity decreases with increasing shear rate ensuring smooth material flow under mechanical stress while maintaining structural integrity after printing. As a wearable device, the hairlike device must endure various forces encountered during normal activities, such as combing or handling hair. Therefore, it is important for a hairlike device to be able to withstand various forces. For reliable application, a device must possess recovery properties from deformation. We tested the performance of the hairlike device under cyclic tensile loading and single tensile loading. The hairlike device exhibited mechanical robustness with high stretchability and tensile cyclability, which is beneficial for real-world applications. Successive cyclic tensile tests with a maximum strain of 10% were conducted for the hairlike device. After cyclic loading, we tested the skin impedance of the hairlike device on the wrist. The hairlike device showed stable electrical performance after 10, 50 and 100 cycles of loading (Fig. 3f). The hairlike device is also highly stretchable with an ultimate strain up to 200% (Fig. 3g).

High-fidelity long-term EEG recording with hairlike device

High-quality EEG recording is crucial for both clinical and research-based neurological applications, including the diagnosis of neurological disorders and the development of brain-machine interfaces (BMIs)^{21,22}. EEG recording offers a noninvasive and efficient method for monitoring brain electrophysiological activities. It provides good temporal resolution that is essential for accurately capturing rapid neural dynamics that is vital for diagnosing conditions such as epilepsy²³, sleep disorders²⁴, brain injuries²⁵, as well as for advancing BMIs, which rely on precise neural signal interpretation to control external devices. Achieving highly effective recording of EEG signals is particularly challenging due to the inherently weak nature of the signals, which have amplitudes in the microvolt range²⁶. Additionally, dense hair on the scalp introduces significant interference, complicating the acquisition of clear and accurate readings²⁷. For EEG, signal quality critically depends on the device's ability to conform closely to the skin. This close conformity ensures optimal contact between the electrodes and the scalp, which is essential for capturing the faint electrical signals generated by brain activity. Any gap can significantly degrade signal quality by increasing impedance and increasing interference from external noise²⁸. Owing to the excellent adhesion performance of the bioadhesive layer and the flexibility and stretchability of the encapsulation layers and hydrogel electrode layer, the hairlike device achieves excellent conformability and compliance with the scalp, even in the presence of dense hair. The hairlike device design ensures that there is minimal interference from hair, allowing the device to maintain intimate contact with the scalp. The robust adhesion prevents any shifting or lifting of the electrodes, while the flexible materials conform to the contours of the scalp, ensuring consistent signal acquisition. As a result, the hairlike device can capture high-quality EEG signals. To validate the efficacy of our hairlike EEG recording device, we conducted a proof-of-

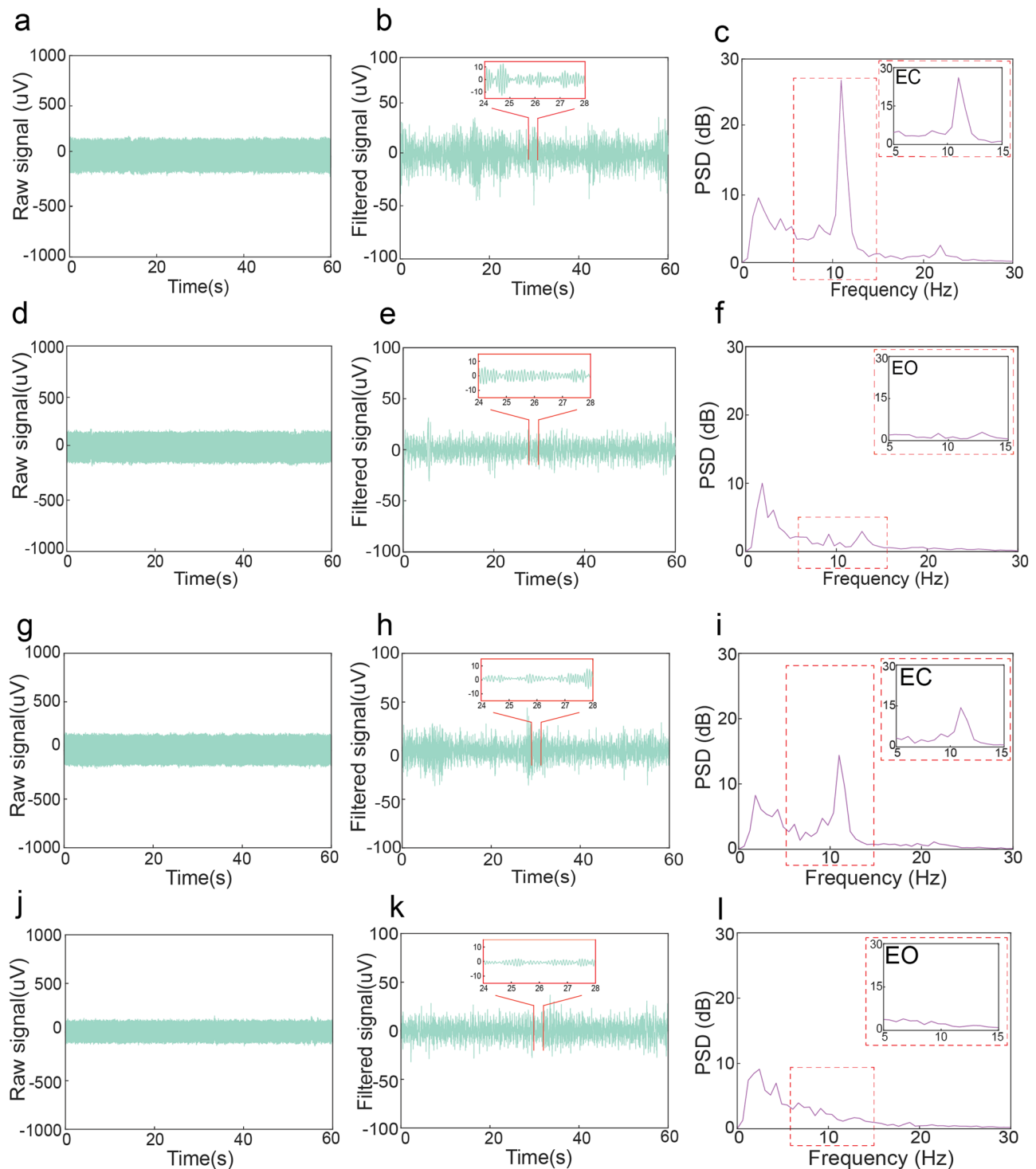


Fig. 4 | High-fidelity chronic EEG signal monitoring from hairy scalp using hairlike electrodes and conventional gold electrodes. **a** EEG raw signal recorded by hairlike electrodes in eyes-closed paradigm. **b** EEG rhythms after filtering in 1–40 Hz range. Subset image: filtered alpha wave signal (8–12 Hz). **c** Power spectral density analysis (PSDA) for EEG signals in (a). **d** EEG raw signal recorded by hairlike electrodes in eyes open paradigm. **e** EEG rhythms after filtering in 1–40 Hz range. Subset image: filtered alpha wave signal (8–12 Hz). **f** PSDA for EEG signals in (d).

g EEG raw signal recorded by conventional gold electrodes in eyes-closed paradigm. **h** EEG rhythms after filtering in 1–40 Hz range. Subset image: filtered alpha wave signal (8–12 Hz). **i** Power spectral density analysis (PSDA) for EEG signals in (g). **j** EEG raw signal recorded by conventional gold electrodes in eyes open paradigm. **k** EEG rhythms form (j) after filtering in 1–40 Hz range. Subset image: filtered alpha wave signal (8–12 Hz). **l** PSDA for EEG signals in (j).

concept study focusing on EEG alpha activity, recorded from the occipital region of a hairy scalp. This area is particularly significant for generating alpha waves, which are typically observed when individuals are in a relaxed state with their eyes closed²⁹. We recorded EEG signals in both eyes-open

and eyes-closed states, using the hairlike device (Fig. 4). The recordings revealed clear differences between the signals detected in these two paradigms. In the eyes-closed states (Fig. 4a–c and Supplementary Fig. 7a), the power spectral density analysis (PSDA) (Fig. 4c) showed a pronounced

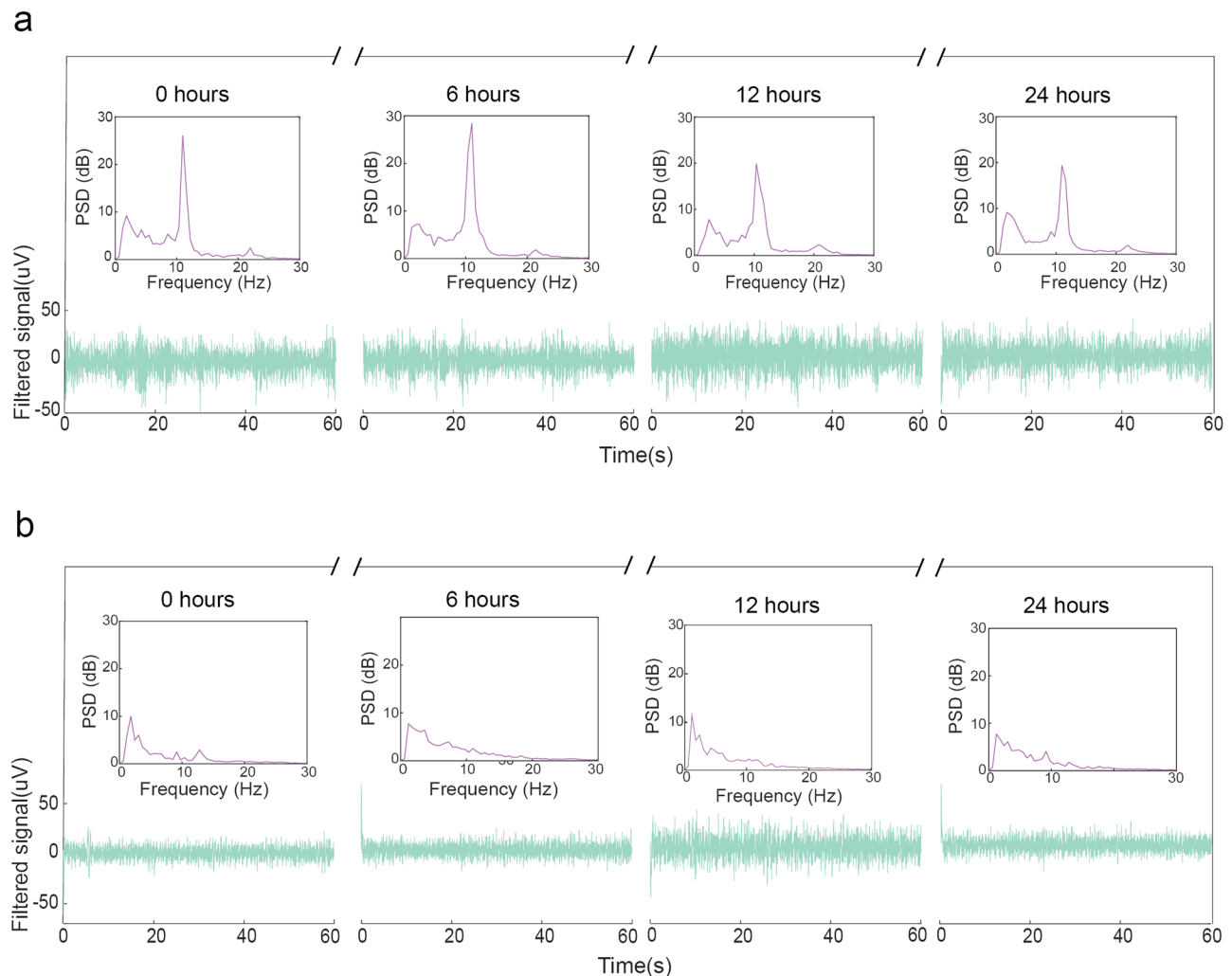


Fig. 5 | Chronic EEG recording using hairlike electrodes. EEG signals recorded in eyes-closed paradigm (a) and eyes-open paradigm (b) after 0, 6, 12 and 24 hours after wearing the hairlike electrodes. The graphs show discernable peak at 10 Hz in eye closed state (a) and no peak at eyes open state (b).

alpha rhythm with a clear central peak around 10 Hz, a characteristic feature of alpha rhythms. Alpha rhythms typically range from 8 to 12 Hz and are associated with a state of relaxed wakefulness³⁰ with reduced visual processing and a more introspective state of mind. Alpha waves are most prominent when the visual cortex is idle, such as when the eyes are closed³⁰, allowing for a clearer detection of these brain waves. In contrast, during the eyes-open state (Fig. 4d-f and Supplementary Fig. 7b), the PSDA (Fig. 4f) showed an absence of alpha rhythm, consistent with the known suppression of alpha waves when the eyes are open, as the brain shifts its activity towards processing visual information and external stimuli. The clear central peak around 10 Hz observed in the PSDA of eyes closed state highlights the hairlike device's ability to accurately capture EEG alpha rhythms. For comparative analysis, we recorded EEG signals from the occipital region using a commercial gold electrode with EEG gel (Fig. 4g-l). This comparison was conducted to benchmark the performance of the hairlike device against a conventional EEG recording standard. The results demonstrated that the hairlike device effectively captured high-quality EEG signals, exhibiting fidelity comparable to, and in some instances surpassing, that of the commercial gold electrodes.

In addition, the hairlike device enabled high-fidelity recording of EEG signals over an extended period, maintaining reliable performance for over 24 hours of continuous wearing (Fig. 5). This long-term stability is attributed to the device's excellent electrical stability, superior mechanical properties, and robust contact with the scalp. EEG signals were recorded upon initial placement of the electrode on the scalp, following which the subjects

engaged in their normal daily activities. Subsequent EEG recordings were collected at 3-hour, 6-hour, and 12-hour intervals. The subjects maintained their regular sleep schedules and sleeping positions overnight. On the following day, after 24 hours of continuous wear, EEG signals were recorded again. The EEG alpha waves recorded at various time points showed no notable degradation in quality. The recordings at different time spans consistently demonstrated high fidelity, with clear patterns characterized by a peak frequency around 10 Hz in the eyes-closed state (Fig. 5a) and no discernible peak in the eyes-open state (Fig. 5b). The consistency of recorded signals across varying time spans strongly underscores the robustness of the hairlike device for long-term EEG monitoring.

Discussion

We successfully demonstrated design and fabrication of high-performance flexible device for long-term high-fidelity EEG recording from hairy scalp. As-prepared hairlike device was able to form stable connection with the skin providing a long-lasting and stable interface impedance. Moreover, the thin, flexible and lightweight structure of the device makes it comfortable to wear and the skin preparation free attachment makes it more convenient for application. The design allows discreet integration with the natural look eliminating social stigma. The elimination of motion artifacts and stable position of the hairlike device makes it a highly effective and reliable medium for the high-fidelity capture of EEG signals with continuous wearing. This technology holds promise for use in consumer health and wellness products, enabling the development of advanced wearable devices

that can monitor mental health³¹, stress levels³², and cognitive functions³³ discreetly. It could also be integrated into brain-computer interface (BCI) systems, enhancing their usability and comfort, thereby expanding their application in fields such as assistive technology for individuals with disabilities, virtual reality (VR) experiences, and even enhancing human-computer interaction in everyday tasks.

Materials and Methods

Materials

Polydimethylsiloxane (PDMS) (SYLGARD™ 186) was obtained from Dow Corning. Poly(3,4-ethylenedioxythiophene): polystyrene sulfonate (PEDOT: PSS) was obtained from Agfa-Gevaert. Dimethyl sulfoxide (DMSO), ethanol, acrylic acid (AA), ethanol, benzophenone, α -ketoglutaric acid, N-(3-dimethylaminopropyl)-N'-ethylcarbodiimide hydrochloride, and N-hydroxysuccinimide, were obtained from Sigma-Aldrich. Hydrophilic polyurethane (PU) (HydroMed D3) was obtained from AdvanSource Biomaterials.

Methods

Preparation of encapsulation and electrode ink

PDMS encapsulating ink was prepared by mixing its part A and part B in 10:1 ratio followed by a thorough mixing in a centrifugal mixer (AR-100, Thinky). For hairlike devices in various colors, part A of PDMS ink was mixed with biocompatible dyes in a centrifugal mixer (AR-100, Thinky) to provide desired color before being cured with part B of PDMS.

To prepare the conductive ink, a 6 w/v% solution of (PEDOT:PSS) was first formulated by dissolving solid PEDOT:PSS pallet in a mixture of deionized water and (DMSO) at a volume ratio of 85:15 (DI water:DMSO). The solution was thoroughly homogenized and then filtered through a 10 μ m polypropylene syringe filter to ensure a uniform PEDOT:PSS suspension. The PEDOT:PSS suspension was combined with a 10 w/w% PU solution in ethanol prepared with a volume ratio of 95:5 (ethanol: DI water). The polymer concentration ratio was maintained at 1:1.5 (PEDOT:PSS to PU). This mixture was filtered again through a 10 μ m polypropylene syringe filter followed by a thorough mixing in a centrifugal mixer (AR-100, Thinky) to prepare a homogeneous conductive ink.

Development of adhesive

The adhesive was prepared using a modified method described in Wu et al.¹⁹. 25% (w/w%) hydrophilic polyurethane (PU) was developed by dissolving polyurethane polymer to the solvent (95% ethanol, 5% DI water). The precursor solution was developed by mixing 19.5 v/v% DI water, 27.5 v/v% ethanol, 25.5 v/v% PU and 25.5 v/v% acrylic acid (AA) respectively. 0.1 w/v% of α -Ketoglutaric acid and 1.1 w/v% of Benzophenone were added to the precursor solution. The mixture was agitated at 200 rpm for 15 minutes in an orbital shaker to allow the materials to dissolve completely. The mixture was then crosslinked under UV light for 180 minutes. During this process, benzophenone served as the photoinitiator, creating radical sites within the PU. These radicals then reacted with acrylic acid, promoting the formation of PU-integrated PAA chains¹⁹. The crosslinked material was then purified through dialysis, initially in 99.5% ethanol for 24 hours (ethanol was replaced after 12 hours), followed by immersion in DI water for another 24 hours (DI water was replaced after 12 hours). The purified PU-PAA was transferred into a beaker and dried in an oven at 70°C for 72 hours. Dried PU-PAA was redissolved into 80% ethanol solution at a concentration of 20 w/w%. The mixture was stirred at 200 rpm at an orbital shaker to allow the material to completely dissolve to form core adhesive and mixed at a ratio of 92.5:7.5 with solution containing 33.3 w/v% of N-(3-dimethylethylamino-propyl)-N'-ethylcarbodiimide hydrochloride and 33.3 w/v% N-hydroxysuccinimide in 70% ethanol solution. This combined solution was mixed with 25 w/w% PU at a 20:3 (v/v) to form the printable ink.

3D printing fabrication of hairlike devices

The designed paths for the hairlike devices were generated using computer-aided design (CAD) drawings in DXF format. These drawings were then

converted into compatible codes to command the x-y-z motion of the printer head via the printer's built-in DXF conversion package (Nordson EFD). The printing paths were custom-designed, allowing independent movement in the x, y, and z directions to align the layers precisely.

Glass substrates, treated with Rain-X water repellent, were used for fabricating hairlike devices. PDMS layers were printed using the prepared PDMS ink, which was loaded into 5 mL syringe barrels fitted with 100 μ m nozzles. These layers were then cured at 125 °C for 15 minutes³⁴. For the electrode layers, the prepared conductive ink was used, also loaded into 5 mL syringe barrels with 100 μ m nozzles. During the printing process, the syringe barrels were connected to an UltimiusPlus dispenser (Nordson EFD) to apply pressure, while the 3D printer precisely moved the printing head along the designed paths. The dispenser's on/off function was controlled by the 3D printer, enabling precise ink deposition along the specified printing paths.

Electrical Characterization

The electrical skin impedance of the hairlike device was measured both on the wrist and on the scalp. The skin impedance was measured using a potentiostat equipped with a frequency response analyzer (Autolab PGSTAT204, Metrohm) using two-electrode system. Two electrode setup was used as EEG signal represents the potential difference between two electrodes and two-electrode setup used for impedance measurement aligns with recording method of EEG data. The distance between two electrodes was ~2 cm and a Cu electrode (10 mm x 10 mm) was used as the reference electrode. For gold electrode (diameter 9 mm), the impedance was measured on both wrist and scalp using a commercial EEG gel. The impedance measurement was conducted at 10 mV with a frequency range of 1–100 kHz. To ensure that two-electrode setup demonstrates a similar performance as three-electrode setup, the impedance measurement with two-electrode setup was compared with conventional three-electrode setup in PBS solution (Supplementary Fig. 8). Although the overall impedance of electrodes in PBS is lower than those on skin due to a better electrode-electrolyte interface in aqueous solution, there was no obvious difference between two-electrode and three-electrode setup (Supplementary Fig. 8).

Rheological, interfacial adhesion and mechanical characterization

Rheological measurements of conductive ink and bioadhesive were performed with Discovery HR-2 hybrid rheometer (TA instruments, New Castle, DE) using 15 mm diameter sand-blasted parallel plates with a constant gap of 300 μ m, at a temperature of 23°C. Viscosity was measured as a function of shear rate at a range of shear rates spanning from 0.01 to 1000 s⁻¹.

The interfacial adhesion on skin tissue was measured through a 90° peeling process using a mechanical testing machine (CellScale) with perpendicular delamination rate of 1 mm/s. The simple stretching measurement of hairlike device was conducted at the rate of 1 mm/s and cyclic loading was conducted at a rate of 0.5 mm/s using CellScale mechanical testing machine. For the measurement of ultimate strain of bioadhesive, dog-bone shaped samples (10 mm in gauge length, 4 mm in width and 0.2 mm in thickness) were subject to deformation at a constant rate of 1 mm/s.

Electroencephalogram (EEG) recording through hairy scalp

Two healthy subjects with dense hair participated in the EEG recordings. The scalp areas chosen for electrode placement were wetted with wet towels before electrode application. The hairlike electrodes were placed at the occipital position. The devices were connected to an Intan 1024ch recording controller (Intan Technologies) via FFC cables and a custom-made PCB board for signal acquisition. An Intan RHD 2132 amplifier was used to amplify the recorded signals. EEG recordings were conducted with a 20-kHz sampling rate, utilizing a 60-Hz notch filter and a Butterworth band-pass filter ranging from 1 Hz to 40 Hz. The reference electrodes were applied on the earlobe. EEG signals were captured under two conditions to investigate the device's performance: 1) with subjects in a relaxed state with their eyes

closed; and 2) with subjects in a relaxed idle state with their eyes opened. After the initial placement of the hairlike electrodes, the subjects wore them continuously for 24 hours. EEG signals were recorded at multiple intervals: initially after device placement, then at 6 hours, 12 hours, and 24 hours.

Electromyography (EMG) recording from muscle

To test the versatility of hairlike electrode, hairlike electrode was attached to the skin of bicep brachii muscles and connected to an Intan recording controller (Intan technologies) and a custom-made PCB board for acquiring EMG signals. The recorded data is shown in Supplementary Fig. 9.

Human test protocols

All human tests were approved by The Pennsylvania State University, Institutional Review Board protocol 00022808 and informed written consent was obtained from all subjects participating in this study.

Data analysis of EEG recording

The EEG data was analyzed with MATLAB (R2023b, MathWorks). The recording data was filtered using Butterworth bandpass filters from 1–40 Hz range. For further analysis of alpha wave, the signal was filtered in a similar method from 8–12 Hz frequency range. After that, custom-written code was used for PSDA (p Welch function in MATLAB) to observe the relaxed and wakeful states.

Statistical analysis

OriginPro 2023 software was used to assess the statistical significance of all comparison studies in this work. In the statistical analysis between two data groups, two-sided unpaired *t*-test was used with the threshold of $****P \leq 0.0001$. One way Anova comparison test was conducted with the threshold of $*P < 0.05$.

Data Availability

All data are available in the main text or the supplementary materials. Additional raw data is available from the corresponding author upon request.

Received: 12 September 2024; Accepted: 20 January 2025;

Published online: 18 March 2025

References

- Pedrosa, P. et al. Alginate-based hydrogels as an alternative to electrolytic gels for rapid EEG monitoring and easy cleaning procedures. *Sens Actuators B Chem* **247**, 273–283 (2017).
- Wang, C. et al. On-skin paintable biogel for long-term high-fidelity electroencephalogram recording. *Sci. Adv.* **8** (2022).
- Buzsáki, G., Anastassiou, C. A. & Koch, C. The origin of extracellular fields and currents — EEG, ECoG, LFP and spikes. *Nat. Rev. Neurosci.* **13**, 407–420 (2012).
- Tatum, W. O. Long-Term EEG Monitoring. *J. Clin. Neurophysiol.* **18**, 442–455 (2001).
- Constant, I. & Sabourdin, N. The EEG signal: a window on the cortical brain activity. *Paediatr. Anaesth.* **22**, 539–552 (2012).
- Tian, Q. et al. Hairy-Skin-Adaptive Viscoelastic Dry Electrodes for Long-Term Electrophysiological Monitoring. *Adv. Mater.* **35** (2023).
- Miyamoto, A. et al. Inflammation-free, gas-permeable, lightweight, stretchable on-skin electronics with nanomeshes. *Nat. Nanotechnol.* **12**, 907–913 (2017).
- Wang, C., He, K., Li, J. & Chen, X. Conformal electrodes for on-skin digitalization. *SmartMat* **2**, 252–262 (2021).
- Gao, D., Parida, K. & Lee, P. S. Emerging Soft Conductors for Bioelectronic Interfaces. *Adv. Funct. Mater.* **30** (2020).
- Abo-Zahhad, M., Ahmed, S. M. & Abbas, S. N. State-of-the-art methods and future perspectives for personal recognition based on electroencephalogram signals. *IET Biom* **4**, 179–190 (2015).
- Wang, L.-F., Liu, J.-Q., Yang, B. & Yang, C.-S. PDMS-Based Low Cost Flexible Dry Electrode for Long-Term EEG Measurement. *IEEE Sens. J.* **12**, 2898–2904 (2012).
- Tallgren, P., Vanhatalo, S., Kaila, K. & Voipio, J. Evaluation of commercially available electrodes and gels for recording of slow EEG potentials. *Clin. Neurophysiol.* **116**, 799–806 (2005).
- Gao, K.-P. et al. Wearable Multifunction Sensor for the Detection of Forehead EEG Signal and Sweat Rate on Skin Simultaneously. *IEEE Sens. J.* **20**, 10393–10404 (2020).
- Ahmed, S., Momin, M., Ren, J., Lee, H. & Zhou, T. Self-Assembly Enabled Printable Asymmetric Self-Insulated Stretchable Conductor for Human Interface. *Adv. Mater.* **36** (2024).
- Xu, S., Ahmed, S., Momin, M., Hossain, A. & Zhou, T. Unleashing the potential of 3D printing soft materials. *Device* **1**, 100067 (2023).
- Zhou, T. et al. 3D printable high-performance conducting polymer hydrogel for all-hydrogel bioelectronic interfaces. *Nat. Mater.* **22**, 895–902 (2023).
- Uslu, E. et al. Enhancing Robustness of Adhesive Hydrogels through PEG-NHS Incorporation. *ACS Appl. Mater. Interfaces* **15**, 50095–50105 (2023).
- Yuk, H. et al. Dry double-sided tape for adhesion of wet tissues and devices. *Nature* **575**, 169–174 (2019).
- Wu, S. J. et al. A 3D printable tissue adhesive. *Nat. Commun.* **15**, 1215 (2024).
- Guimarães, C. F., Gasperini, L., Marques, A. P. & Reis, R. L. The stiffness of living tissues and its implications for tissue engineering. *Nat. Rev. Mater.* **5**, 351–370 (2020).
- Casson, A., Yates, D., Smith, S., Duncan, J. & Rodriguez-Villegas, E. Wearable Electroencephalography. *IEEE ENG. MED. BIOL.* **29**, 44–56 (2010).
- Mahmood, M. et al. Fully portable and wireless universal brain-machine interfaces enabled by flexible scalp electronics and deep learning algorithm. *Nat. Mach. Intell.* **1**, 412–422 (2019).
- Noachtar, S. & Rémi, J. The role of EEG in epilepsy: A critical review. *Epilepsy Behav* **15**, 22–33 (2009).
- Behzad, R. & Behzad, A. The Role of EEG in the Diagnosis and Management of Patients with Sleep Disorders. *J. Behav. Brain Sci.* **11**, 257–266 (2021).
- Rapp, P. E. et al. Traumatic Brain Injury Detection Using Electrophysiological Methods. *Front. Hum. Neurosci.* **9** (2015).
- Scheer, H. J., Sander, T. & Trahms, L. The influence of amplifier, interface and biological noise on signal quality in high-resolution EEG recordings. *Physiol. Meas.* **27**, 109–117 (2006).
- Etienne, A. et al. Novel Electrodes for Reliable EEG Recordings on Coarse and Curly Hair. *42nd Annual Intl Conf. of the IEEE Engineering in Medicine & Biology Society (EMBC)* 6151–6154 (IEEE, 2020).
- Wu, H. et al. Materials, Devices, and Systems of On-Skin Electrodes for Electrophysiological Monitoring and Human-Machine Interfaces. *Adv. Sci.* **8** (2021).
- Moini, J. & Piran, P. Cerebral cortex. in *Functional and Clinical Neuroanatomy* 177–240 (Elsevier, 2020).
- Blinowska, K. & Durka, P. Electroencephalography (EEG). In *Wiley Encyclopedia of Biomedical Engineering* (Wiley, 2006).
- Simmatias, L., Russo, E. E., Geraci, J., Harsmen, I. E. & Samuel, N. Technical and clinical considerations for electroencephalography-based biomarkers for major depressive disorder. *npj Mental Health Res* **2**, 18 (2023).
- Katmah, R. et al. A Review on Mental Stress Assessment Methods Using EEG Signals. *Sensors* **21**, 5043 (2021).
- Bell, M. A. & Cuevas, K. Using EEG to Study Cognitive Development: Issues and Practices. *J. Cogn. Dev.* **13**, 281–294 (2012).
- Momin, M. et al. 3D-printed flexible neural probes for recordings at single-neuron level. *Device* 100519 (2024).

Acknowledgements

The authors acknowledge Yuqi Wang for help with rheological experiments and analysis. This work is supported by the National Institutes of Health

(1R01HL171633 to T.Z.). T.Z. acknowledges support from the Department of Engineering Science and Mechanics, the Materials Research Institute, and the Huck Institutes of the Life Sciences at the Pennsylvania State University. T.Z. acknowledges support from Oak Ridge Associated Universities (ORAU). T.Z. and C.-C.K. acknowledge the support of the National Taipei University of Technology-Penn State Collaborative Seed Grant Program (NTUT-PSU-113-01).

Author contributions

T.Z. conceived the project. T.Z. and C.-C.K. secured funding. S.A., M.M. and T.Z. designed the experiments. S.A. and M.M. designed and fabricated the devices. S.A., M.M. conducted electrical and mechanical characterization. S.A. conducted rheology, AFM and FTIR experiments. S.A., M.M., J.R., H.L., B.A., L.-P.H., A.P., and L.V. performed the wearable device experiments. S.A., M.M., J.R. conducted data analysis. S.A., M.M., B.A., and L.-P.H. prepared the figures for the manuscript with input from all authors. S.A. drafted the manuscript. T.Z. revised the manuscript with input from all authors.

Competing interests

The authors declare no competing interests.

Additional information

Supplementary information The online version contains supplementary material available at

<https://doi.org/10.1038/s44385-025-00009-x>.

Correspondence and requests for materials should be addressed to Chi-Ching Kuo or Tao Zhou.

Reprints and permissions information is available at <http://www.nature.com/reprints>

Publisher's note Springer Nature remains neutral with regard to jurisdictional claims in published maps and institutional affiliations.

Open Access This article is licensed under a Creative Commons Attribution-NonCommercial-NoDerivatives 4.0 International License, which permits any non-commercial use, sharing, distribution and reproduction in any medium or format, as long as you give appropriate credit to the original author(s) and the source, provide a link to the Creative Commons licence, and indicate if you modified the licensed material. You do not have permission under this licence to share adapted material derived from this article or parts of it. The images or other third party material in this article are included in the article's Creative Commons licence, unless indicated otherwise in a credit line to the material. If material is not included in the article's Creative Commons licence and your intended use is not permitted by statutory regulation or exceeds the permitted use, you will need to obtain permission directly from the copyright holder. To view a copy of this licence, visit <http://creativecommons.org/licenses/by-nc-nd/4.0/>.

© The Author(s) 2025